ISSN 0208-7774 TRIBOLOGIA 1/2021 p. 39–51
DOI: 10.5604/01.3001.0015.4899

Stanisław STRZELECKI*

STATIC CHARACTERISTICS OF OFFSET 8-LOBE JOURNAL BEARINGS

CHARAKTERYSTYKI STATYCZNE 8-POWIERZCHNIOWYCH ŁOŻYSK ŚLIZGOWYCH Z PRZESUNIĘTYMI SEGMENTAMI

Key words: hydrodynamic lubrication, multilobe offset journal bearings, static characteristics.

Abstract: The 8-lobe journal bearings have found application in the bearing systems of spindles of grinding machines. The design of bearings and the large number of lobes and oil grooves assures good cooling conditions of bearing. These bearings can be manufactured as the bearings with cylindrical, non-continuous operating surfaces separated by six lubricating grooves, bearings with the pericycloidal shape of the bearing bore, and as offset journal bearing.
This paper presents the results of the computation of static characteristics of an offset 8-lobe journal bearing operating under the conditions of an aligned axis of journal and bush, adiabatic oil film, and at the static equilibrium position of journal. Different values of bearing length to diameter ratio, relative clearance, and lobe relative clearance were assumed. Reynolds' energy and viscosity equations were solved by means of an iterative procedure. Adiabatic oil film, laminar flow in the bearing gap, and aligned orientation of journal in the bearing were considered.

Słowa kluczowe: smarowanie hydrodynamiczne, wielopowierzchniowe łożyska ślizgowe offset, charakterystyki statyczne

Streszczenie: Łożyska ślizgowe 8-powierzchniowe stosowane są w układach łożyskowania wrzecion szlifierek. Konstrukcja tych łożysk i znaczna liczba powierzchni ślizgowych oraz rowków smarowych zapewniają dobre warunki chłodzenia. Łożyska te mogą być wykonywane z segmentami o powierzchni kołowej, zarysie nieciągłym lub ciągłym; z przesuniętymi segmentami, a powierzchnie ślizgowe są oddzielone rowkami smarowymi.
Artykuł przedstawia obliczenia charakterystyk statycznych łożysk 8-powierzchniowych z przesuniętymi segmentami pracujących w warunkach równoległych osi czopa i panewki i statycznego położenia równowagi czopa. Założono różne wartości względnej długości łożyska, luzu łożyskowego i względnego luzu segmentu. Równanie Reynoldsa, energii i lepkości rozwiązano metodą różnic skończonych autorskim kodem numerycznym. Przyjęto adiabatyczny i laminarny model przepływu środka smarowego w szczelinie smarowej.

INTRODUCTION

Multilobe journal bearings are applied in different types of high speed rotating machines. They assure good thermal conditions and stability of operation **[L. 1–4]**. The requirements of more effective and robust design of these bearings cause that there is continuation of researches into their performances **[L. 5–14]**. The bearings with the offset lobes, e.g., offset-halves **[L. 15–18]** are used in accelerating turbo-gearboxes on the input stage **[L. 15]**. These bearings are usually 2-lobe ones **[L. 15, 16]** with horizontally displaced half bushes and they operate in one direction of rotation. Displacement of both halves causes the need for a reduction in oil flow and the application of segment relative clearance

* ORCID: 0000-0001-5030-5249. Łódź, Poland.

ψ_s equal 2 to 3. In these offset-halves bearings, the circle inscribed in the bore profile touches the end of the convex gap of the bearing **[L. 15, 17]**.

The properties of good stability and convenient cooling conditions allow the application of multilobe journal bearings in the design of grinding spindles **[L. 11–13]** too. These bearings can be designed as the bearings of non-continuous **[L. 3]** or continuous (pericycloid) **[L. 3]** bore profile. In multilobe bearings, the temperature rise is comparatively high, and it causes the problems that, in some cases, result in damage to the bearing. The foundation for the safe operation of such bearings at proper oil film temperature is the full knowledge of bearing static and dynamic characteristics. Static characteristics are determined by the static equilibrium position angles, minimum oil film thickness, maximum oil film temperature, and pressure, oil flow and friction loss, and they are very important in evaluating of the journal bearing performances.

Referring to the advantages of offset-halves bearing, it is interesting to check the static characteristics of the 8-lobe journal bearing **[L. 18, 19]** with offset lobes. Such information can be very useful for both designers and users of multilobe journal bearings of different applications.

This paper presents the results of the calculations of static characteristics of 8-lobe journal bearings with the offset lobes and operating at different length to diameter ratios, bearing and lobe relative clearances, as well as at different rotational speeds of spindle. A numerical method by means of finite differences was applied for the simultaneous solution of geometry, Reynolds and energy, and viscosity equations on the assumption of adiabatic oil film. Some results were obtained for diathermal oil film **[L. 19]**.

GEOMETRY, REYNOLDS AND ENERGY EQUATIONS

On the assumption of the parallel axis of journal and bearing sleeve, the geometry of oil film gap of multilobe journal bearing (**Fig. 1**) is described by Eqn. (1); the first term of this equation describes the geometry of multilobe bearing **[L. 1–3]**.

$$\bar{H}(\phi) = \bar{H}_{Li}(\phi) - \varepsilon \cdot \cos(\phi - \alpha) \tag{1}$$

where: $\bar{H}$ = h/(R – r) – dimensionless oil film thickness, h – oil film thickness (m), R, r – sleeve and journal radius (m), α – attitude angle, (°), ε – relative eccentricity, φ – peripheral co-ordinate, (°), i – number of lobes

$$\bar{H}_{Li}(\phi) = \psi_{si} + (\psi_{si} - 1) \cdot \cos(\phi - \gamma_i) \tag{2}$$

where: γ_i – angle of lobe centre point, (°), ψ_{si} – lobe relative clearance ($\psi_{si} = \bar{H}_{max}/\bar{H}_{min}$), γ – peripheral co-ordinate of the segment centre.

The journal bearing performances for adiabatic model of oil film can be determined by the numerical solution of the oil film geometry, Reynolds, energy and viscosity equations on the assumption of static equilibrium position of the journal **[L. 1**, **3]**. The oil film pressure distribution was obtained from Eqn. (3).

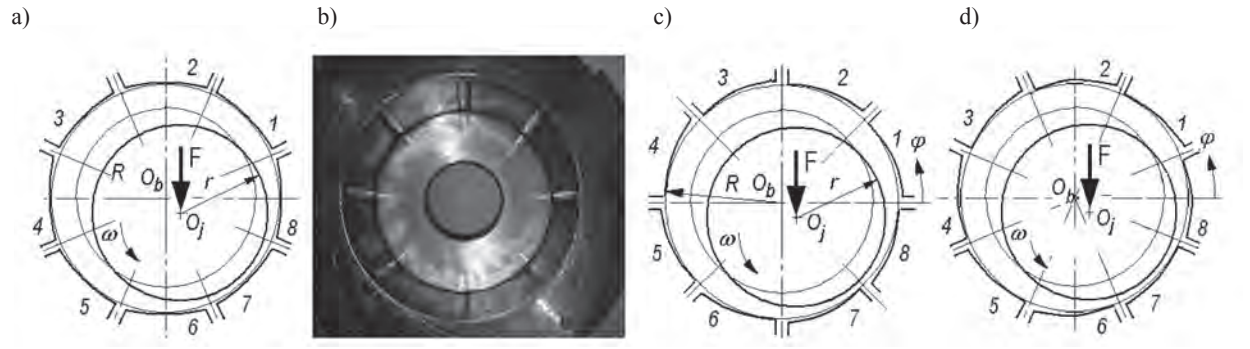

Fig. 1. 8-lobe journal bearings: a) classic, b) general view, c) and d) offset 8-lobe geometry (c – load between lobes – LBL, d – load on lobe – LOL); F – bearing load, O_b, O_j – bearing and journal centre, r – radius of journal R_l – radius of lobe, ω – angular velocity [3, 12, 18]

Rys. 1. Łożysko 8-powierzchniowe: a) klasyczne, b) widok ogólny, c), d) geometria łożyska 8-powierzchniowego offset (c – obciążenie między segmentami – LBL, d – obciążenie na segment – LOL); F – obciążenie łożyska, O_b, O_j – środek łożyska i czopa, r – promień czopa R_l – promień segmentu, ω – prędkość kątowa **[3, 12, 18]**

$$\frac{\partial}{\partial\phi}\left(\frac{\bar{H}^3}{\bar{\eta}}\frac{\partial\bar{p}}{\partial\phi}\right)+\left(\frac{D}{L}\right)^2\frac{\partial}{\partial\bar{z}}\left(\frac{\bar{H}^3}{\bar{\eta}}\frac{\partial\bar{p}}{\partial\bar{z}}\right)=6\frac{\partial\bar{H}}{\partial\phi}+12\frac{\partial\bar{H}}{\partial\varphi} \tag{3}$$

where: $\bar{p}$ – dimensionless oil film pressure, $\bar{p} = p\psi^2/(\eta\omega)$, p – oil film pressure (MPa), (m), D, L – bearing diameter and length (m), t – time (sec), $\bar{z}$ – axial co-ordinates, $\phi = \omega t$ – dimensionless time, $\bar{\eta}$ – dimensionless viscosity, ψ – bearing relative clearance, $\psi = \Delta R/R$ (‰), ΔR – bearing clearance, $\Delta R = R - r$ (m).

It has been assumed for the pressure region that on the bearing edges the oil film pressure $p(\phi, z) \geq 0$ and in the regions of negative pressure, $p(\phi, z) = 0$. The oil film pressure distribution computed from Eqn. (3) was put in the transformed energy equation **[L. 3–14]** to obtain the temperature and viscosity distributions. Temperature $T(\phi, z)$ on the boundaries ($z = \pm L/2$) was determined by means of the parabolic approximation **[L. 3]**. The Exponential equation of viscosity was applied **[L. 3]**.

Oil film temperature distribution for the adiabatic model of oil film was obtained from Eqn. (4).

$$\frac{\bar{H}}{Pe}\left[\frac{\partial^2\bar{T}}{\partial\phi^2}+\left(\frac{D}{L}\right)^2\frac{\partial^2\bar{T}}{\partial\bar{z}^2}\right]+\left[\frac{\bar{H}^3}{12\bar{\eta}}\frac{\partial\bar{p}}{\partial\phi}-\frac{\bar{H}}{2}\right]\frac{\partial\bar{T}}{\partial\phi}+$$
$$\left(\frac{D}{L}\right)^2\frac{\bar{H}^3}{12\bar{\eta}}\frac{\partial\bar{p}}{\partial\bar{z}}\frac{\partial\bar{T}}{\partial\bar{z}}=-\frac{\bar{H}^3}{12\bar{\eta}}\left[\left(\frac{\partial\bar{p}}{\partial\phi}\right)^2+\left(\frac{D}{L}\right)^2\left(\frac{\partial\bar{p}}{\partial\bar{z}}\right)^2\right]-\frac{\bar{\eta}}{\bar{H}} \tag{4}$$

where: $\bar{T}$ – dimensionless oil film temperature, $\bar{T} = T/T_0$, T: temperature of oil film, (°C), T_0: temperature of supplied oil, (°C), c – specific heat of lubricant (J/kg°C), ρ – density of lubricant (kg/m^3).

In the case of diathermal model of oil film, the temperature distribution was found from the solution of Eqn. (5) and additional equations of heat conduction **[L. 3**, **19]**.

$$\frac{1}{2\bar{\eta}}\frac{\partial\bar{p}}{\partial\phi}\left(\bar{y}^2-\bar{H}\bar{y}\right)+\left(1-\frac{\bar{y}}{\bar{H}}\right)\frac{\partial\bar{T}}{\partial\phi}=\bar{\eta}K_T\left[\frac{1}{2\bar{\eta}}\frac{\partial\bar{p}}{\partial\phi}\left(2\bar{y}-\bar{H}\right)-\frac{1}{\bar{H}}\right]+\frac{1}{Pe}\frac{\partial^2\bar{T}}{\partial\bar{y}^2} \tag{5}$$

where: K_T – thermal coefficient, $K_T = \omega \cdot \eta_0/(c_t \cdot \rho \cdot T_0 \cdot \psi^2)$, $\bar{y}$ – dimensionless radial coordinate, Pe – Peclet number, $Pe = \rho c\omega r^2/h$.

Developed program of numerical calculation **[L. 3]** solves all above-given equations.

RESULTS OF THEORETICAL INVESTIGATION

Exemplary results of computations were obtained for the following data: bearing length to diameter ratio L/D = 0.5, 0.8, 1.0, relative clearance ψ = 0.6, 1.0, 1.2 ‰, lobe relative clearance ψ_s = 1 through 4, and additionally ψ_s = 3.9. Rotational speeds were 1500 through 3000 rpm.

The distributions of pressure and temperature that were obtained for the adiabatic model of oil film are presented in **Figs. 2** through **4** for multilobe 8M and 8OF journal bearings. It is interesting that the distributions of oil film pressure are different on each lobe in both considered types of bearings. In the case of the 8M bearing, the oil film pressure does not occur on the full length of lobe, e.g., **Fig. 3** lobe No. 6 (φ < 225°, 270°>). However, the pressure exists on the full length of each lobe in the case of the 8OF bearing (**Fig. 4** lobe No. 6 (φ < 225°, 270°>).

For comparison purposes, the oil film temperature distributions on the bearing peripheral of 8M bearings were obtained in the case of a diathermal model of oil film at assumed relative eccentricity of journal (ε = 0.4) and for the cylindrical (8C, ψ_s = 1) as well as for the multilobe profile (8M, ψ_s = 2) with the load between lobes (**Fig. 5**); at considered values of lobe relative

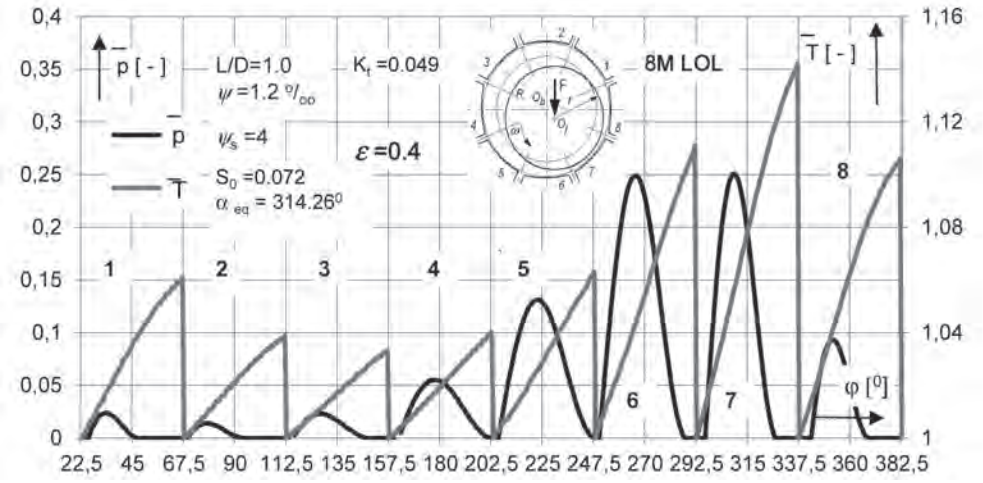

Fig. 2. Oil film pressure and temperature distributions in 8-lobe journal bearing (LOL)
Rys. 2. Rozkład ciśnienia i temperatury w filmie smarowym łożyska 8-powierzchniowego (LOL)

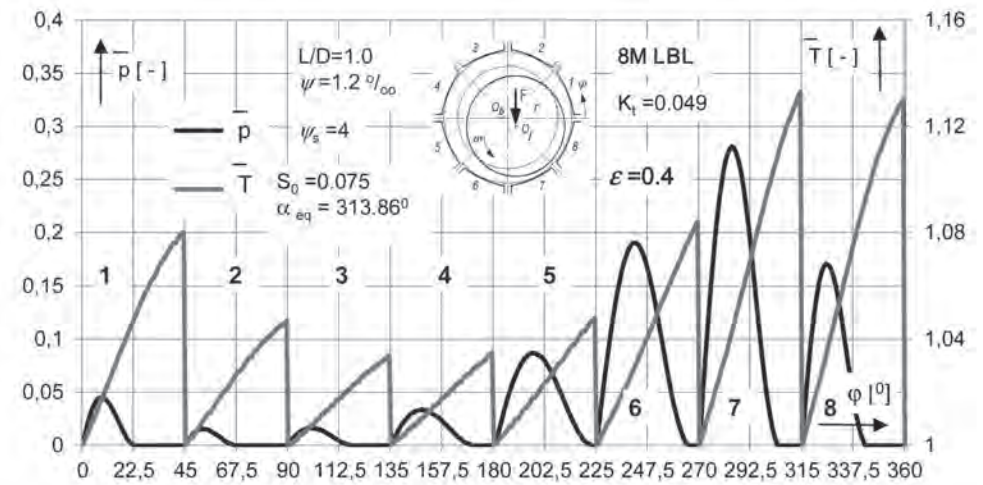

Fig. 3. Oil film pressure and temperature distributions in 8-lobe journal bearing (LBL)
Rys. 3. Rozkład ciśnienia i temperatury w filmie smarowym łożyska 8-powierzchniowego (LBL)

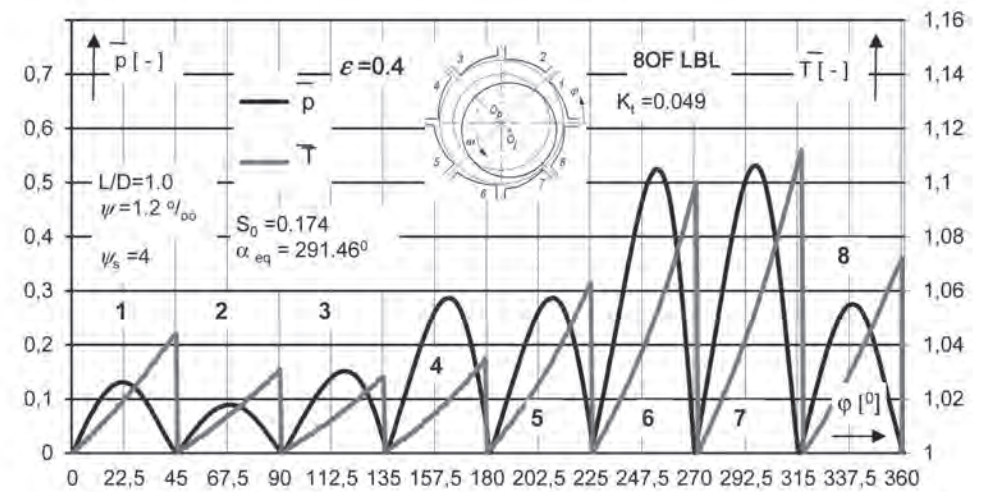

Fig. 4. Oil film pressure and temperature distributions in 8-lobe Offset journal bearing (LBL)
Rys. 4. Rozkład ciśnienia i temperatury w filmie smarowym łożyska 8-powierzchniowego offset (LBL)

clearance, there is small difference in obtained temperature distributions (**Fig. 5a** and **Fig. 5b**). The highest temperatures are generated on lobe No. 8 (e.g., **Fig. 5a**) and the lowest on lobe No. 4; lobe No. 1 shows comparatively high temperatures, because the oil film transfers the heat from lobe No. 8, i.e. the lobe showing the highest temperature.

The diathermal model of oil film **[L. 19]** is more exact than the adiabatic one, but the computation of bearing characteristics for such model takes more time; however, there are small differences in computed parameters of bearing as compare to the adiabatic model.

Figure 6 shows the oil film pressure and temperature distributions on lobe No. 7 (most thermally loaded lobe) of the 8M bearing at assumed journal relative eccentricity. In the case of the bearing with the load on the lobe, the load

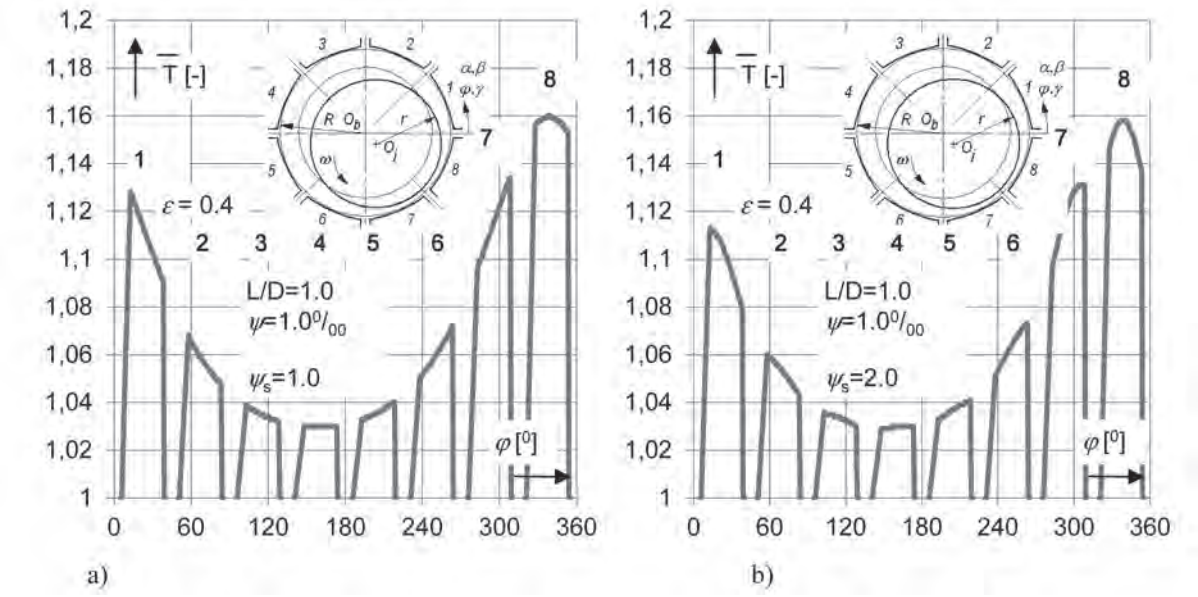

Fig. 5. Oil film temperature distribution in 8-lobe cylindrical (a – 8C LBL) and multilobe journal bearing (b – 8M LBL) journal bearing

Rys. 5. Rozkład temperatury w filmie smarowym łożyska 8-powierzchniowego cylindrycznego (a – 8C LBL) i wielopowierzchniowego (b – 8M LBL)

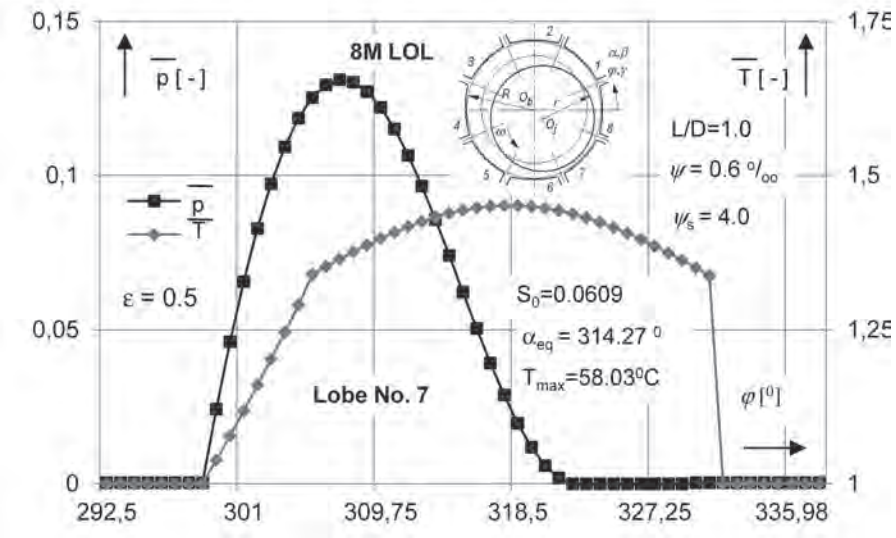

Fig. 6. Oil film pressure and temperature distributions on lobe No. 7 and No. 8 of the 8-lobe journal bearing 8M LOL (most thermally loaded lobe) at assumed journal relative eccentricity; the load on lobe No. 6

Rys. 6. Rozkład ciśnienia i temperatury w filmie smarowym łożyska 8-powierzchniowego na segmencie 7 i 8 łożyska 8-powierzchniowego 8M LOL (najbardziej obciążone cieplnie segmenty) dla założonego przemieszczenia względnego czopa; obciążenie na segmencie nr 6

is directed on lobe No. 6 (**Fig. 1d**); however, for bearings with the load between lobes (8M LBL), the load direction is between the lobes No. 6 and No. 7 (**Fig. 1c**). The maximum oil film temperature is located over the point of nil pressure value (e.g., **Fig. 6**, the peripheral coordinate φ is approximately 320°).

Journal displacements ε and static equilibrium position angles α_{eq} of the different types of 8 lobe journal bearings at assumed lobe relative clearances ψ_{si} are shown in **Fig. 7**. At the assumed value of journal displacement (e.g., ε = 0.6), the larger load capacity is on bearing 8M and the smallest is of bering 8OF (**Fig. 7a**; ψ_s = 3). As for the static

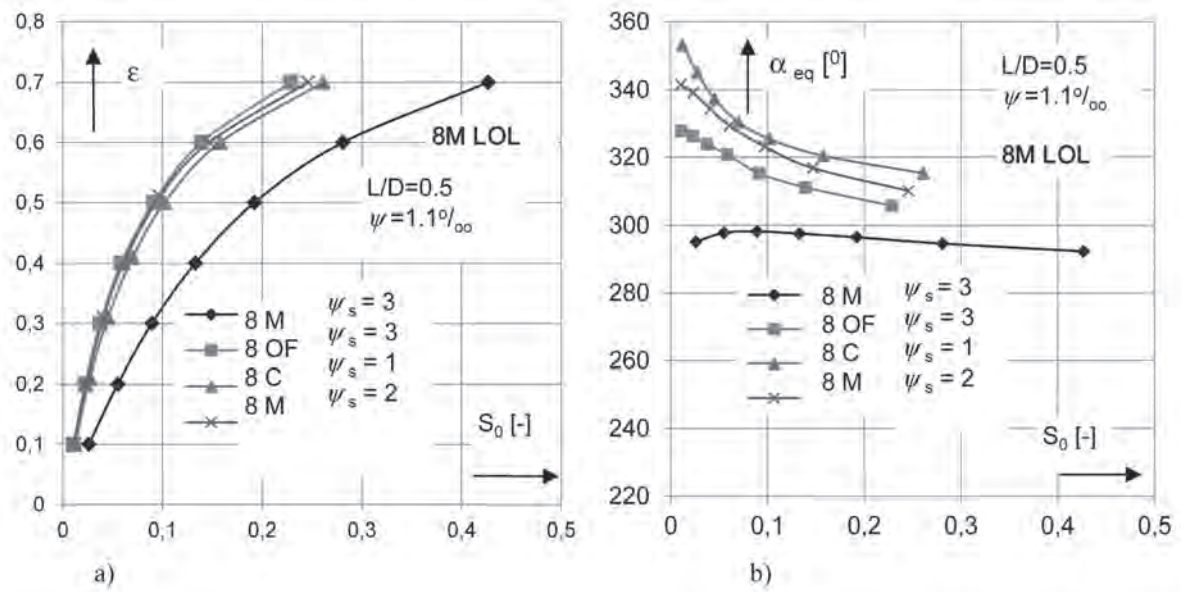

Fig. 7. Journal displacements (a) and static equilibrium position angle (b) of different types of 8 lobe journal bearings versus Sommerfeld number

Rys. 7. Przemieszczenia czopa (a) i kąty statycznego położenia równowagi czopa (b) różnych rodzajów łożysk 8-powierzchniowych w funkcji liczby Sommerfelda

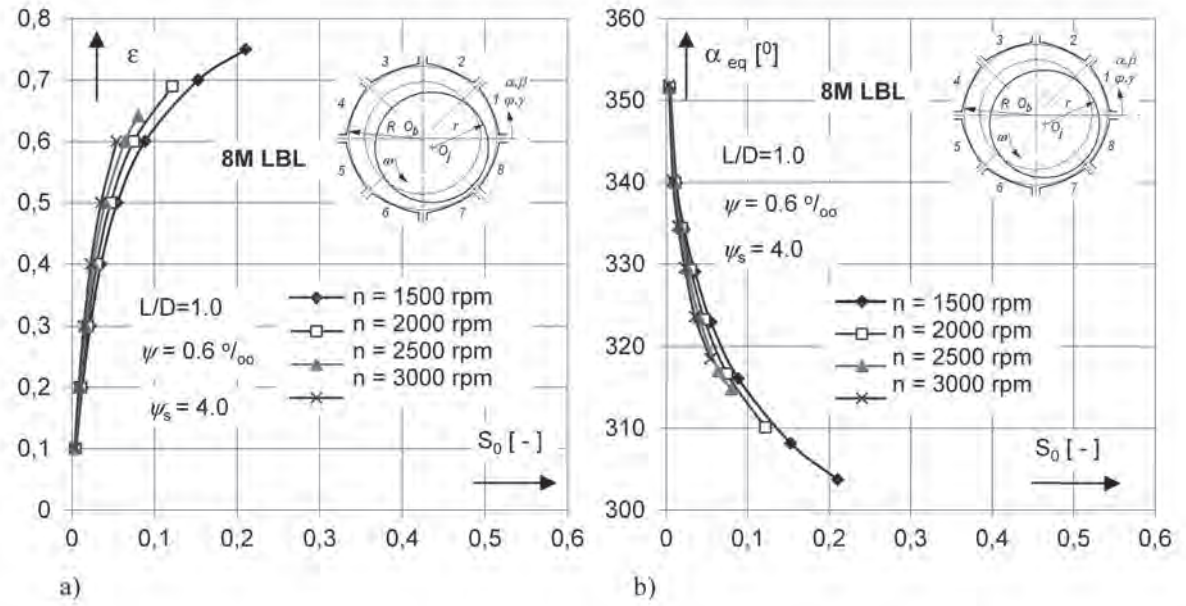

Fig. 8. Effect of rotational speed on the journal displacements (a) and the static equilibrium position angles (b) versus Sommerfeld number

Rys. 8. Wpływ prędkości obrotowej na przemieszczenia czopa (a) i kąty statycznego położenia czopa (b) w funkcji liczby Sommerfelda

equilibrium position angle α_{eq}, the smallest values are on bearing 8M and the largest is on 8C (**Fig. 7b**).

An effect of rotational speed on the journal displacements ε and static equilibrium position angles α_{eq} in the bearing with the load between lobes can be observed in **Fig. 8**. At the assumed journal displacement, an increase in the rotational speed causes the decrease in the load capacity (**Fig. 8a**; e.g., for ε = 0.6, S0 ≈0.09 for 1500 rpm and S0≈0.05 at 3000 rpm). A similar situation exists for the static equilibrium position angle (**Fig. 8b**; e.g., $\alpha_{eq} = 320°$).

The comparison of static equilibrium position angles α_{eq} and maximum oil film temperature T_{max} for the 8OF bearings are presented in **Fig. 9**. There are different arrangements of load with respect to the load direction. Maximum oil film temperature is larger for the bearing with the load on the lobe (**Fig. 9b**).

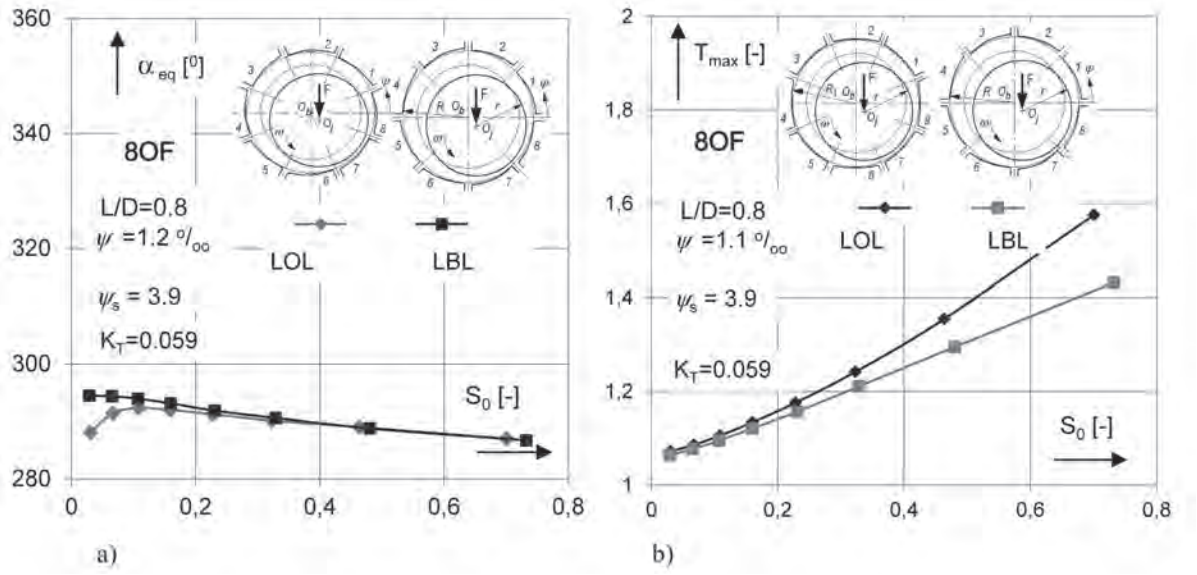

Fig. 9. Comparison of static equilibrium position angles (a) and maximum oil film temperature for two types of offset 8-lobe journal bearings

Rys. 9. Porównanie kątów statycznego położenia równowagi (a) i maksymalnej temperatury w filmie smarowym (b) dla dwóch rodzajów łożysk 8OF

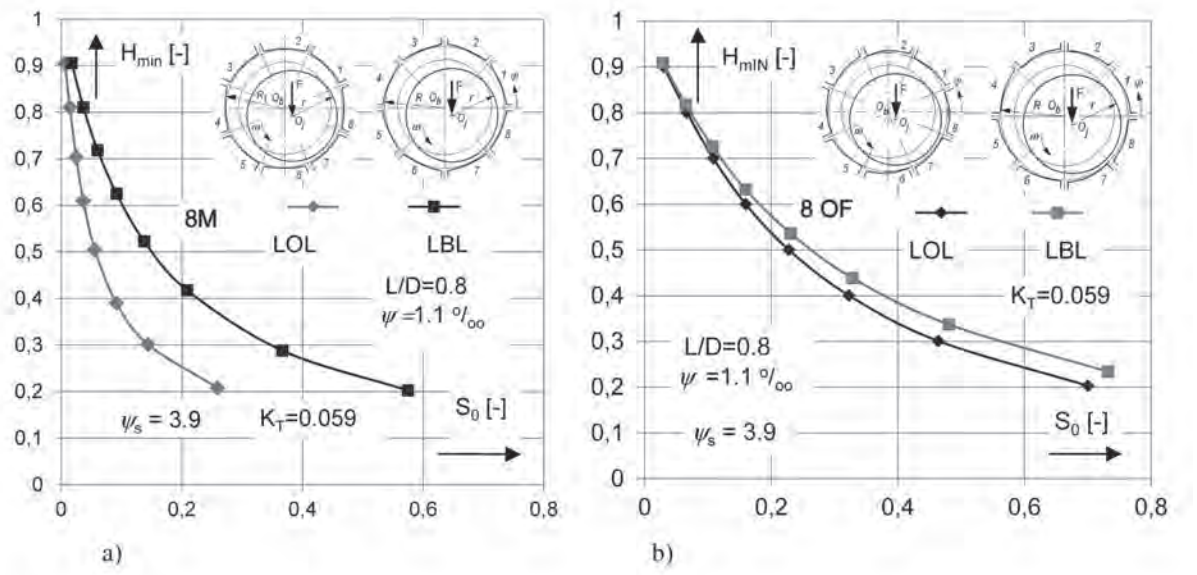

Fig. 10. Comparison of the minimum oil film thickness of two types of 8-lobe journal bearings: a) classic (LOL and LBL), b) offset (LOL and LBL)

Rys. 10. Porównanie minimalnej grubości filmu smarowego dwóch rodzajów łożysk 8-powierzchniowych: a) klasyczne (LOL i LBL), b) offset (LOL i LBL)

A comparison of the minimum oil film thickness of two types of 8-lobe journal bearings [a – classic (8M LOL and LBL), b – (8OF LOL and LBL)] is presented in **Fig. 10**. For the assumed S_0 and load direction, H_{min} is smaller for the bearing 8M (e.g., $S_0 = 0.4$ in **Fig. 10a** and **Fig. 10b** – LOL).

Fig. 11 presents an effect of lobe relative clearance on the oil flow (**Fig. 11a**) and power loss (**Fig. 11b**) for three types of 8-lobe bearings. The largest oil flow is in the 8OF bearing and the smallest is in 8C, particularly in the range of Sommerfeld numbers below 0.05 (**Fig. 11a**). The power loss is the highest for the 8C bearing and the smallest is for 8OF bearing (**Fig. 11b**).

Fig. 12 presents the maximum oil film temperature at the assumed rotational speed of the journal and for different values of bearing relative clearance for the bearing with the load on the lobe. An increase in the bearing clearance causes

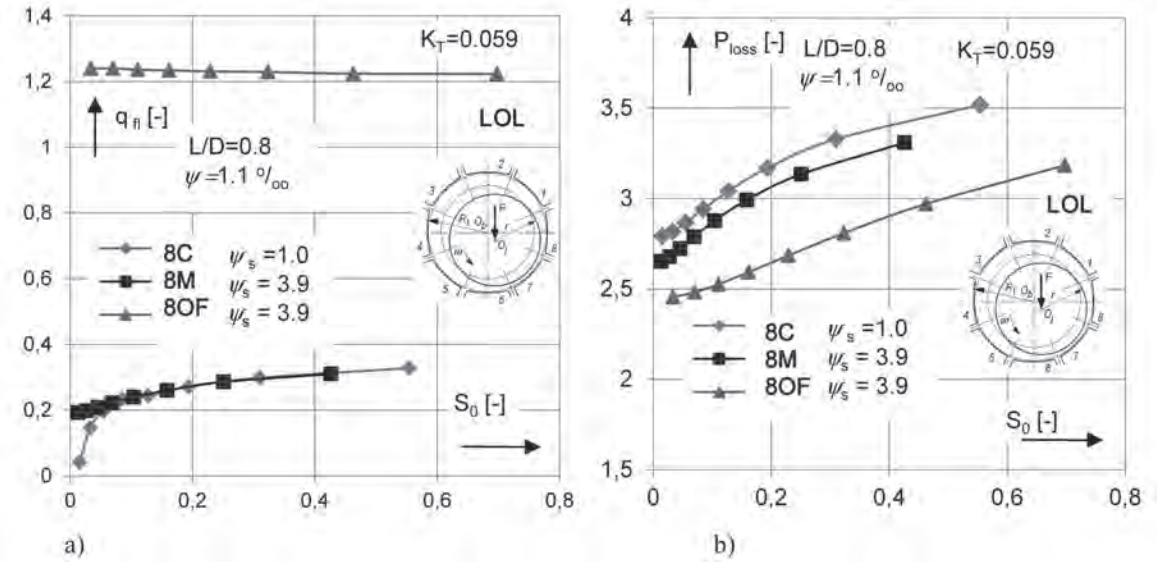

Fig. 11. Effect of lobe relative clearance on the oil flow (a) and power loss (b) versus Sommerfeld number
Rys. 11. Wpływ względnego luzu segmentu na przepływ środka smarowego (a) i straty mocy (b) w funkcji liczby Sommerfelda

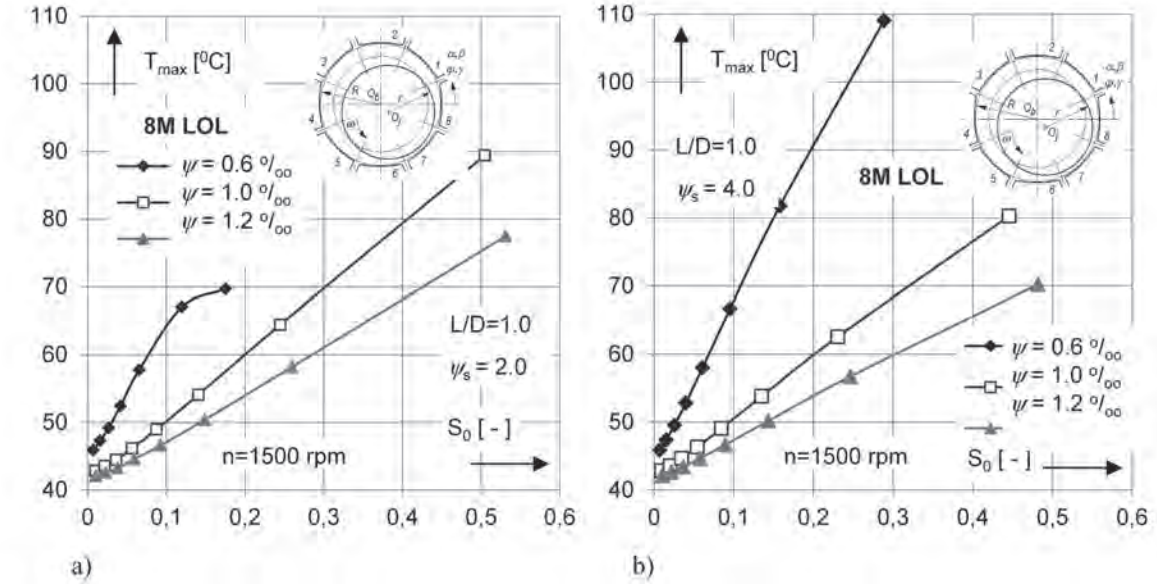

Fig. 12. Maximum oil film temperatures at different values of bearing relative clearance versus Sommerfeld number; lobe relative clearance a – ψ_s = 2.0, b – ψ_s = 4.0
Rys. 12. Maksymalna temperatura filmu smarowego dla różnych wartości względnego luzu łożyskowego w funkcji liczby Sommerfelda; względny luz segmentu a – ψ_s = 2.0, b – ψ_s = 4.0

the decrease in the maximum oil film temperature (e.g., **Fig. 12a** at assumed So = 0.1, maximum oil film temperatures T_{max} = 65°C at ψ = 0.6‰, and T_{max} = 48°C at ψ = 1.2‰).

The effect of rotational speed on the maximum oil film temperature is shown in **Fig. 13**. An increase in the journal rotational speed causes the increase in the maximum oil film temperature in both cases of considered 8-lobe journal bearings, i.e. the bearing with the load on the lobe (**Fig. 13a**) and the load between the lobes (**Fig. 13b**).

Static equilibrium position angles α_{eq} for two types of 8-lobe bearings, i.e. 8M and 8OF with the load directed between the bottom lobes are presented in **Fig. 14** and **Fig. 15**, whre there were assumed the different bearing relative clearance

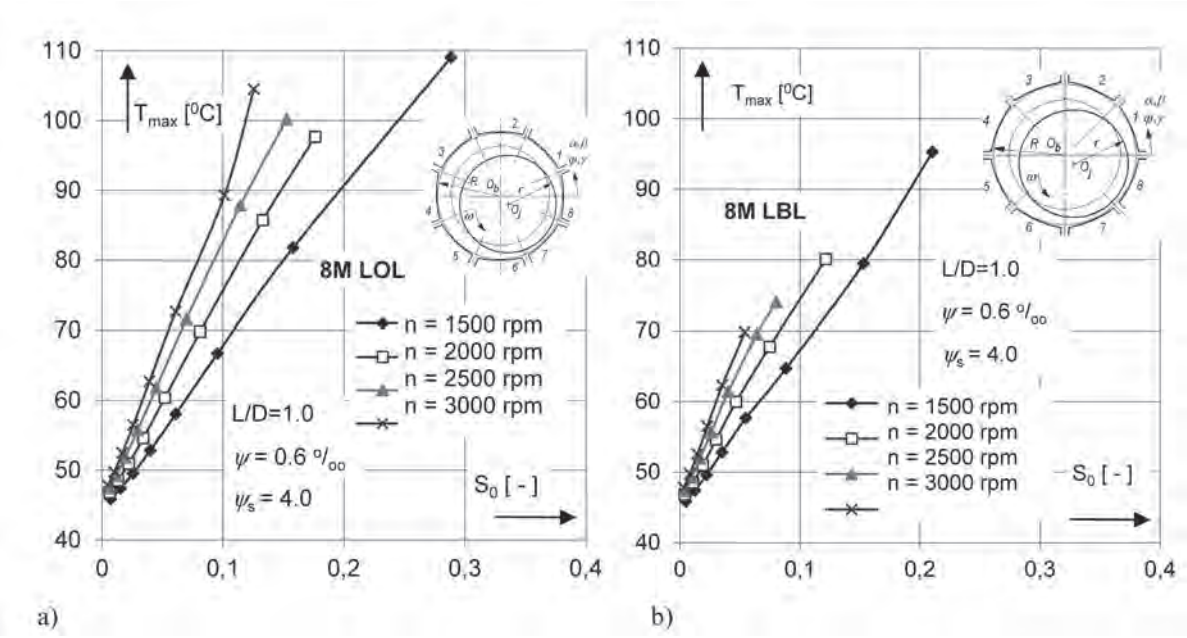

Fig. 13. Effect of rotational speed on the maximum oil film temperature for two types of 8-lobe journal bearings: a) load on the bottom lobe (LOL), b) load between the bottom lobes (LBL)

Rys. 13. Wpływ prędkości obrotowej na maksymalną temperaturę filmu smarowego łożysk 8-powierzchniowych; a) obciążenie na segmencie dolnym (LOL), b) obciążenie miedzy segmentami (LBL)

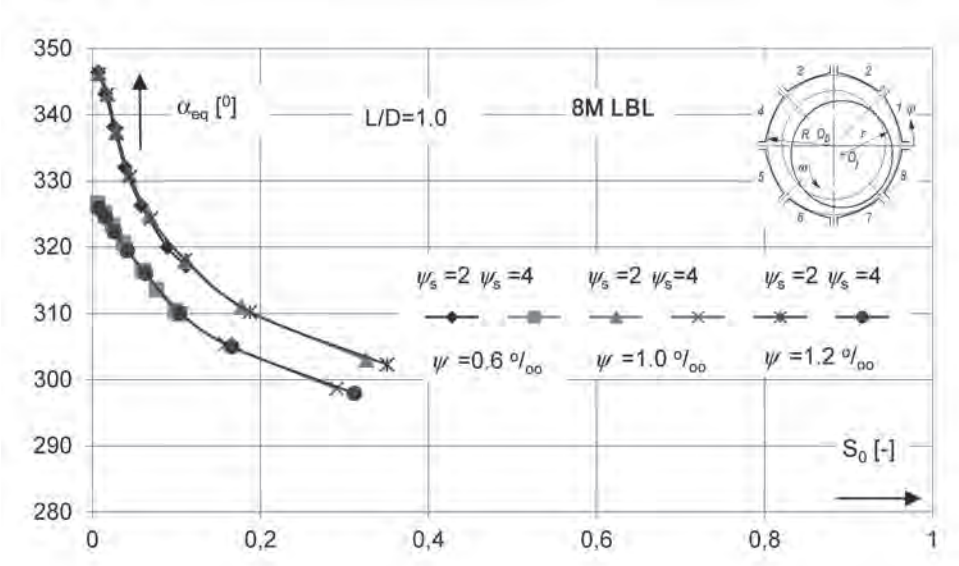

Fig. 14. Effect of relative clearance and lobe relative clearance on the static equilibrium position angles (8 lobe journal bearing 8M LBL)

Rys. 14. Wpływ względnego luzu łożyskowego i względnego luzu segmentu na kąty statycznego położenia równowagi (łożysko 8M LBL)

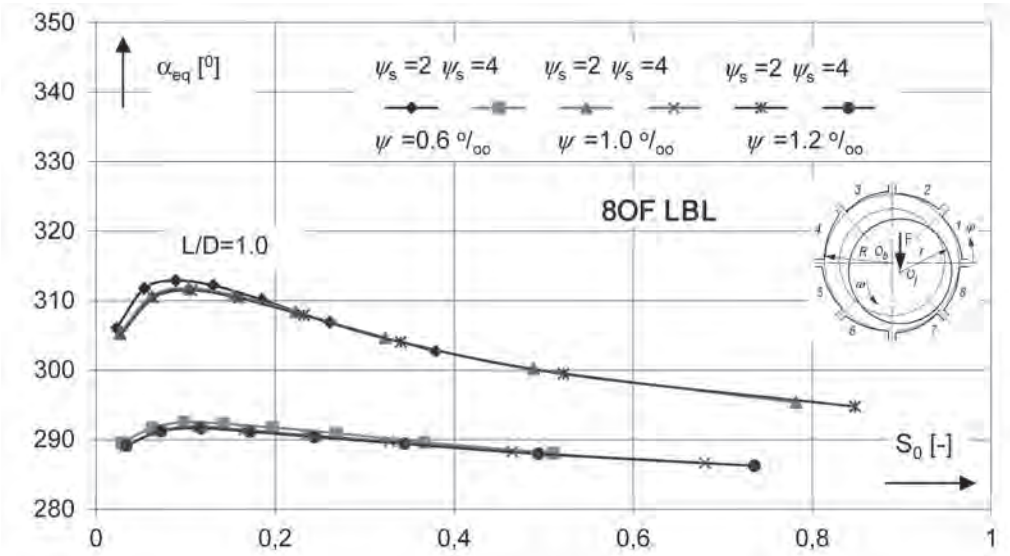

Fig. 15. Effect of relative clearance and lobe relative clearance on the static equilibrium position angles (8OF LBL bearing)
Rys. 15. Wpływ względnego luzu łożyskowego i względnego luzu segmentu na kąty statycznego położenia równowagi (łożysko 8OF LBL)

ψ and lobe relative clearance ψ_s. At larger values of lobe relative clearances ψ_s = 4.0, the static equilibrium position angles α_{eq} are smaller than in the case of $_{si}$ = 2 (**Fig. 14** and **Fig. 15**, e.g., ψ = 0.6‰, and ψ_s = 2 or ψ_s = 4) for considered relative clearances ψ of bearing.

An effect of relative clearance ψ and lobe relative clearance ψ_s on the non-dimensional values of maximum oil film temperature $\bar{T}_{max}$ is given in **Figs. 16** through **18**. There is smaller range of bearing load capacity in the case of the 8M bearing than in 8OF, but it is larger for the 8OF one (e.g., **Fig. 16** and **Fig. 17**). An increase in bearing relative clearance ψ causes the decrease in maximum oil film temperature $\bar{T}_{max}$ for both considered lobe relative clearances ψ_s. At a larger value of lobe relative clearance and at assumed bearing relative clearance, there is small decrease in maximum oil film temperature in the case of 8M and 8OF LOL bearings (**Fig. 16** and **Fig. 18**), but a larger decrease is observed for the 8OF LBL bearing (**Fig. 17**, e.g., S_0 = 0.2 and ψ = 0.6‰ , ψ = 1.0‰, ψ = 1.2‰, there are the different values of $\bar{T}_{max}$ at the lobe relative clearances ψ_s = 2, ψ_s = 4).

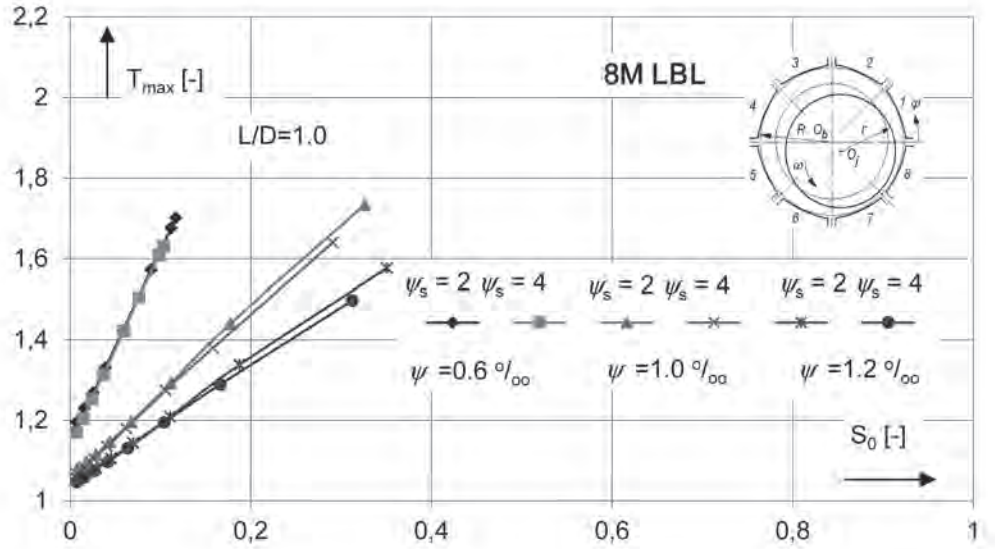

Fig. 16. Effect of relative clearance and lobe relative clearance on the maximum oil film temperature (8 lobe journal bearing 8M LBL)
Rys. 16. Wpływ względnego luzu łożyskowego i względnego luzu segmentu na maksymalną temperaturę filmu smarowego (łożysko 8M LBL)

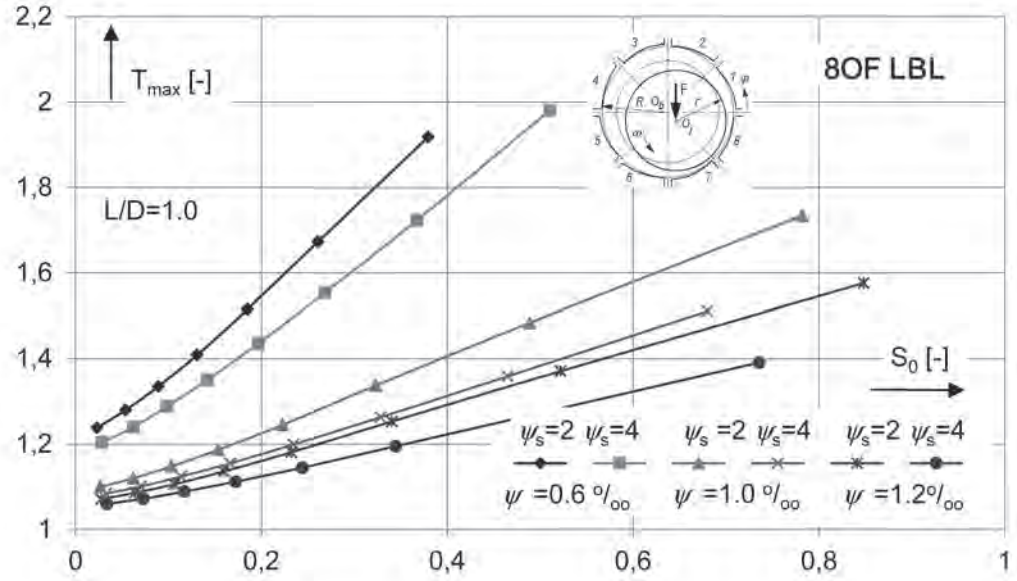

Fig. 17. Effect of relative clearance and lobe relative clearance on the maximum oil film temperature (8 lobe offset journal bearing 8OF LBL)

Rys. 17. Wpływ względnego luzu łożyskowego i względnego luzu segmentu na maksymalną temperaturę filmu smarowego (łożysko offset 8OF LBL)

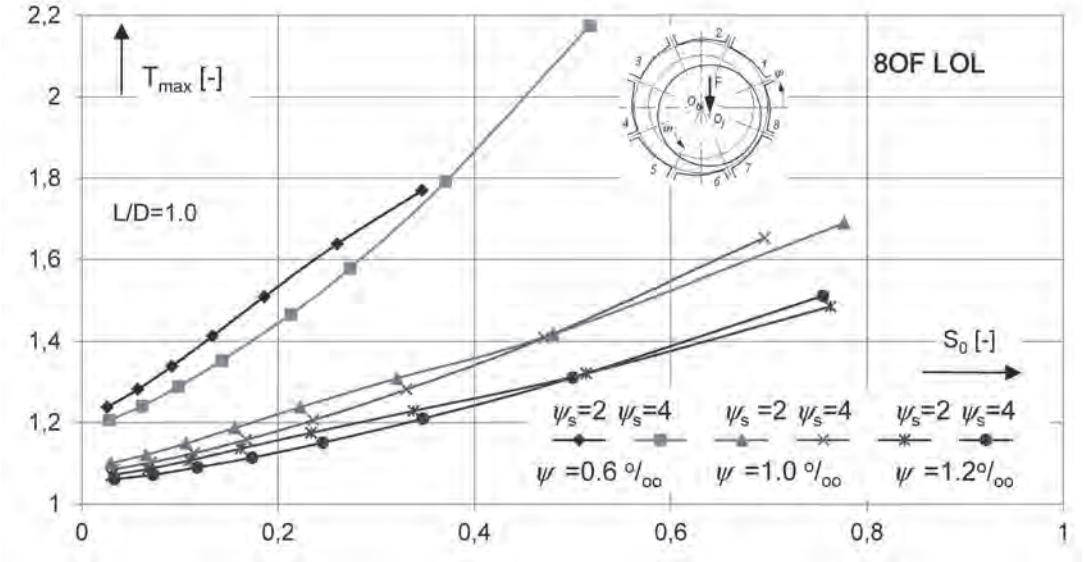

Fig. 18. Effect of relative clearance and lobe relative clearance on the maximum oil film temperature (8 lobe offset journal bearing 8OF LOL)

Rys. 18. Wpływ względnego luzu łożyskowego i względnego luzu segmentu na maksymalną temperaturę filmu smarowego (łożysko offset 8OF LOL)

FINAL REMARKS

The developed code of journal bearings computations that operates in the Windows environment allows for obtaining the static characteristics of the 8-lobe journal bearings including offset types. The results of computation give the basis for the analysis, evaluation, and for the choice of best parameters in the design process of multilobe bearings.

The considered rotational speeds of the journal have a small effect on the displacements of the journal and the static equilibrium position angles; however, it affects the maximum oil film temperatures

The direction of load with regard to the lobes arrangement of the offset 8-lobe bearings affects their static characteristics and, among others, the maximum oil film temperatures of oil film. The bearing geometry parameters, such as the bearing relative clearance and lobe relative clearance, cause the variation in the maximum oil film temperature and in the range of smaller Sommerfeld numbers, these temperatures are smaller for the 8-lobe offset bearing. More exact data on the thermal state of bearings can be obtained for the diathermal model of oil film.

Generally, there is a small effect of the bearing relative clearance on the displacement of journal and static equilibrium position angles. However, a larger effect on these parameters shows the lobe relative clearance.

Minimum oil film thickness at an assumed value of Sommerfeld number is larger for the 8OF bearing than for 8M at any arrangement of bearing lobes in regard to the load direction.

At an increase of lobe relative clearance, the oil flow shows an increase, but there is the decrease in power loss that seems to be important with the point of power savings.

REFERENCES

1. Someya T.: Journal-Bearing Databook, Springer-Verlag Berlin, Heidelberg, 1989.
2. Pinkus O.: Thermal Aspects of Fluid Film Tribology, ASME PRESS, New York 1990.
3. Ghoneam S.M., Strzelecki S.: Thermal Problems of Multilobe Journal Bearings, Meccanica, DO1 10.1007/s11012-006-9004-z, "Meccanica" 41, Springer 2006, pp. 571–579.
4. Chauhan A.: Non-Circular Journal Bearings, Springer International Publishing 2016.
5. Thiery F., Gantasala S., Aidanapaa J-O.: Numerical evaluation of multilobe bearings using the spectral method, "Advances in Mechanical Engineering" 2017, Vol. 9 (7), pp. 1–10.
6. Kumar P. R., Bhaskar K., Hussain M.M.: Analysis of multi lobe journal bearings with surface roughness using finite difference method, IOP Conference Series: Materials Science and Engineering, Vol. 346, Issue 1. 012071, 2018.
7. Biswas N., Pandey K.M.: Transient CFD Analysis of Multi-Lobe Bearings at 60000 RPM for a Gas Turbine, "IACSIT Int. Journal of engineering and Technology" 2011, Vol. 3, No. 5, October.
8. Bhagat C., Roy L.: Steady State Thermo-Hydrodynamic Analysis of two-Axial groove and Multilobe Hydrodynamic Bearings, "Tribology in Industry" 2014, Vol. 36, No. 4, pp. 475–487.
9. Biswas N., Chakraborti P., Saha A., Biswas S.: Performance & stability analysis of a three lobe journal bearing with varying parameters: Experiments and analysis, AIP Conference Proceedings 1754, 030002, 2016, https://doi.org/10.1063/1.4958346.
10. Gorunov L.V., Takmoytsey V.V., Sokolov E.V. , Il'inkov A.V.: Experimental study of pressure fields in a multilobe journal bearing, "Russian Aeronautics" 2015 (Iz. VUZ) Vol. 58, pp. 233–236.
11. Strzelecki S., Someya T.: Static characteristics of the Offset-Halves journal bearing, Proceedings of the VIIth International Symposium on Teratology INTERTRIBO'99, April 27–30, 1999, Stara Lesna, The High Tatras, Slovakia 1999, pp. 289–292.

12. Strzelecki S., Ghoneam S.M.: Stability of Jeffcott rotor operating in offset halves journal bearings, PEDAC, Alexandria Egypt. 14–18.02.2009, ID 123 Conftool.
13. Strzelecki S., Kapusta H.: Dynamic characteristics and stability of 3-lobe offset journal bearing, "Machine Dynamics Problems" 2006 , Vol. 30, No. 4, pp. 131–139.
14. Strzelecki S.: Effect of Bore Profile on the Static and Dynamic Characteristics of 6-Lobe Journal Bearing. Proceedings of 2nd International Symposium on Stability Control of Rotating Machinery. Gdańsk, Poland 2003, pp. 140–149.
15. Strzelecki S., Kapusta H.: Maximum oil film temperature of 8-lobe journal bearing. Proc. of the International Scientific-Technical Conference on Tribology, URAL-TRIBO, 8–12 September 2014, Tschelabinsk, Russia 2014, pp. 18–24.
16. Strzelecki S.: Static and dynamic characteristics of 8-lobe journal bearing, Proc. of Vth International Symposium INTERTRIBO'96, High Tatra, Slovakia 1996, pp. 212–215.
17. Strzelecki S.: Stiffness and damping coefficients of 8-lobe journal bearings, XXIX SYMPOSIUM on VIBRATIONS IN DYNAMICAL SYSTEMS, 21st–23rd of October 2020, Poznań, Vol. 31, No. 3, 2020, 2020321.
18. Strzelecki S.: Maximum Oil Film Temperature in Offset 8-Lobe Journal Bearing, Tribologie Fachtagung. 28–30 September 2020, Goettingen, Germany.
19. Strzelecki S.: Multilobe journal bearings with the lobes of different geometry, 2018 (Non-published).